Communications to the Editor

Electrical Detection of Self-Assembled Polyelectrolyte Multilayers by a Thin Film Resistor

Petra A. Neff,[†] Ali Naji,[‡] Christof Ecker,[§] Bert Nickel,[⊥] Regine v. Klitzing,[§] and Andreas R. Bausch*,[†]

Lehrstuhl für Biophysik-E22, Technische Universität München, Germany; Physik Department-T37, Technische Universität München, Germany; Institut für Physikalische Chemie, Christian-Albrechts-Universität Kiel, Germany; and Department für Physik, Ludwig-Maximilians-Universität München, Germany

Introduction. Despite the broad potential applications of polyelectrolyte multilayers (PEMs), a detailed understanding of the buildup process and the resulting basic physical properties is still elusive. While the multilayer thickness, the water content, the mechanical properties, and the swelling behavior of different PEMs systems have been extensively studied, their electrostatic properties are still not fully determined. PEMs are prepared by the layer-by-layer deposition of polyanions and polycations from aqueous solutions.[1,2] During the adsorption process polyanion/polycation complexes are formed with the previously adsorbed polyelectrolyte layer,[3] leading to a charge reversal.[4] The exchange of counterions by the oppositely charged polyelectrolyte could be the reason for the counterion concentration inside the PEMs to be below the detection limit.[5] Thus, it seems that most of the charges within the PEMs are compensated intrinsically by the opposite polymer charges and not by the presence of small counterions. Related to the intrinsic charge compensation may be the strong interdigitation between adjacent layers found by neutron reflectometry.[6,7] While the potential of the outer PEMs surface is well investigated by electrokinetic

measurements,[4] not much is known about the internal electrostatic properties like ion distribution and mobility. Using a pH-sensitive fluorescent dye, the distribution of protons within the PEMs has been determined.[8] Assuming Debye screening and a constant mobility for all ions within the PEMs, the potential drop within polyelectrolyte films composed of poly(allylamine hydrochloride) (PAH) and poly(sodium 4-styrenesulfonate) (PSS) has been calculated. From these measurements an independent determination of the ionic strength and the dielectric constant was not possible. Recent X-ray fluorescence measurements have been promising in estimating the ion density profile inside the PEMs, giving the total amount of free and condensed ions.[9]

Direct measurements of the potential drop inside the PEMs will be best suited for determining electrostatic properties such as the Debye length or the dielectric constant of the PEMs. The capacitance of the PEMs can be measured by electrochemical methods such as ac voltammetry.[10] Another approach is the use of field effect devices which allows the determination of the surface potential at the sensor/electrolyte interface. Obviously, the surface potential variations measured by such a device are strongly dependent on screening effects inside the adjacent phase. The deposition of PAH/PSS as well as poly(L-lysine)/DNA multilayers and even DNA hybridization have been detected by such devices.[11-13] However, a physical model is needed to relate the quantitative response of the sensors to the dielectric properties and ion mobility inside the PEMs.

Here we show that a silicon-on-insulator (SOI) based thin film resistor is suited to monitor in real time the buildup of polyelectrolyte multilayers consisting of the strong polyelectrolyte PSS and the weak polyelectrolyte PAH. The sheet resistance of the field effect device is sensitive to variations of the potential ψ_S at the silicon oxide surface. The deposition of the differently charged polyelectrolytes results in defined potential shifts, which decrease with the number of layers deposited. Applying a capacitor model, the observed decrease can be quantitatively explained by assuming reduced electrostatic screening by mobile charges inside the PEMs compared to the bulk medium outside.

* To whom correspondence should be addressed: e-mail abausch@ph.tum.de.
  † Lehrstuhl für Biophysik-E22, Technische Universität München.
  ‡ Physik Department-T37, Technische Universität München.
  § Christian-Albrechts-Universität Kiel.
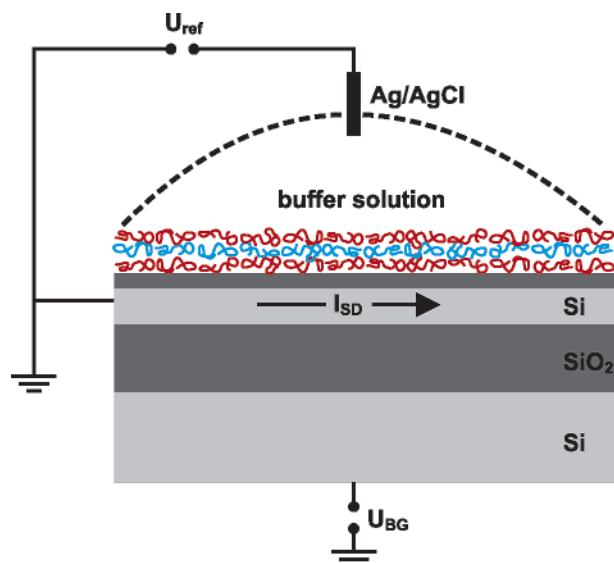 ⊥ Ludwig-Maximilians-Universität München.

Figure 1. Sketch of the setup and the measurement geometry. Silicon is shown in light gray and silicon oxide in dark gray. From top to bottom: native oxide (1−2 nm), conducting top silicon (30 nm), buried oxide (200 nm), bulk silicon (675 μm). A voltage is applied between the source and the drain contacts, and the resulting current I_{SD} is measured yielding the sheet resistance of the device. The carrier concentration in the top silicon layer is tuned by the backgate voltage U_{BG}. The potential of the electrolyte solution is controlled by a Ag/AgCl reference electrode. A microfluidic device allows the rapid exchange of electrolyte solution.

Experimental Section. All chemicals including PSS (MW 70 000) and PAH (MW 60 000) were purchased from Sigma-Aldrich. Buffers were prepared using ultrapure water (Millipore, France) with a resistivity >18 MΩ·cm. 5 mg/mL polyelectrolyte solutions were prepared by direct dissolution in 10 mM Tris buffer at pH 7.5 containing 50 and 500 mM NaCl.

The sensor chips were fabricated from commercially available silicon-on-insulator (SOI) wafers (ELTRAN, Canon) using standard lithographic methods and wet chemical etching as described in detail elsewhere.[14] The top silicon layer of these wafers was 30 nm thick and slightly doped with boron (10^{16} cm^{-3}). Metal contacts were deposited in an electron beam evaporation chamber (20 nm Ti, 300 nm Au). After evaporation, the sensor chips were cleaned using acetone and 2-propanol. The chips were glued into a chip carrier, and the contacts were Au wire bonded to the carrier. Afterward, the chips were encapsulated with a silicone rubber to insulate the contacts from the electrolyte solution. The sheet resistance of the device is dependent on the potential ψ_S of the SiO$_x$/PEMs interface and was measured as described elsewhere.[15] The potential ψ_S was then calculated from the sheet resistance by a calibration curve of the specific SOI wafer. A flow chamber was mounted on top of the sensor, and a Ag/AgCl reference electrode was used to control the potential of the electrolyte solution and for calibration. The setup and the measurement geometry are shown schematically in Figure 1. First, the sensor was equilibrated in the buffer solution. Next, a calibration measurement was performed as shown elsewhere.[15] PAH and PSS solutions were injected twice into the flow chamber to ensure full coverage of the sensor surface, starting with the positively charged PAH. After obtaining a stable sensor signal, the chamber was rinsed twice with buffer of the same salt concentration as the polyelectrolyte solutions. As soon as a stable signal was obtained, the next polyelectrolyte solution was injected and the procedure was repeated up to 20 times. The sheet resistance of the thin film resistor was monitored continuously during the
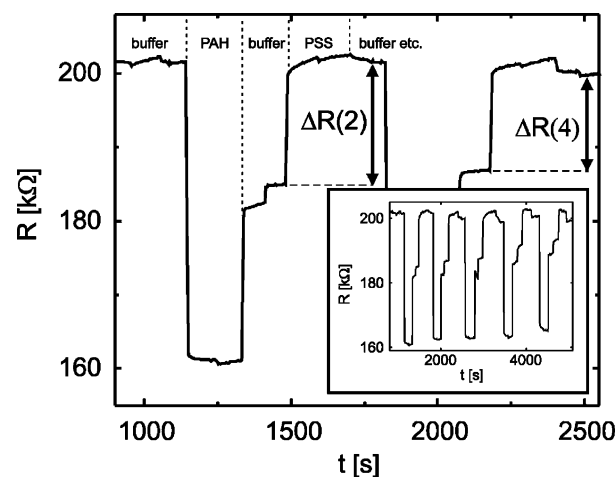

Figure 2. Deposition of four PEMs from 50 mM NaCl is shown in detail. The sheet resistance was monitored continuously during the buildup process. For each deposition step the polyelectrolyte solution was injected twice. When a stable signal was obtained, the sensor was rinsed twice with buffer. The resistance change ΔR between adjacent deposition steps of PAH and PSS is indicated for two and four adsorbed layers. The potential change between adjacent deposition steps $\Delta\psi_S$ was calculated from ΔR using the calibration data. The inset displays the subsequent adsorption of 10 layers.

multilayer deposition. In separate experiments the thickness of the deposited polyelectrolyte films was determined by an ellipsometer (Optrel, Multiscope, Berlin, Germany) in electrolyte solution. Care was taken to perform the preparation of multilayers as close as possible to the conditions employed for the deposition on the thin film resistors. The ellipsometry was carried out in the same buffer solutions used for the sample preparation.

Results and Discussion. During the layer-by-layer deposition of the polycation PAH and the polyanion PSS by alternating buffer exchange, the sheet resistance of the SOI sensor was continuously observed. The deposition of the alternately charged polyelectrolytes results in defined responses of the sensor (Figure 2). The adsorption of PAH decreases the sheet resistance corresponding to an increased ψ_S (the potential directly at the SiO$_x$/PEMs interface) as positive charges bind to the surface. The subsequent adsorption of the negatively charged PSS increases the resistance and thus decreases ψ_S. As the SOI sensor exhibits also a pH sensitivity,[15] the large potential shift between the PAH deposition and the subsequent washing step can be attributed to the pH of the PAH solution which is decreased to 6.4 by dissolution of the weak polyelectrolyte in the buffer of pH 7.5. The deposition of up to 20 monolayers was observable by the field effect device. The potential change between adjacent deposition steps $\Delta\psi_S$ was determined from the measured sheet resistance using the calibration data and is plotted against the number of adsorbed monolayers, as shown in Figure 3. It can clearly be seen that the potential jumps $\Delta\psi_S$ decrease with the number of layers deposited. This is in contrast to electrokinetic studies, where the surface potential at the outer PEMs/electrolyte interface is measured and the steps remain constant over a large number of deposited layers.[4] The observed decrease of $\Delta\psi_S$ can be explained by adapting a capacitor model.[10,16] The sensor device with the adsorbed PEMs is modeled assuming three separate domains: (i) the sensor device, which is modeled as a one-dimensional silicon/silicon oxide structure characterized by its capacitance per area C_S; (ii) the PEMs consisting of N monolayers each of thickness d; (iii) the electrolyte solution outside the PEMs, where a diffuse electrical double layer is formed at the PEMs/electrolyte interface (Figure 4). To proceed
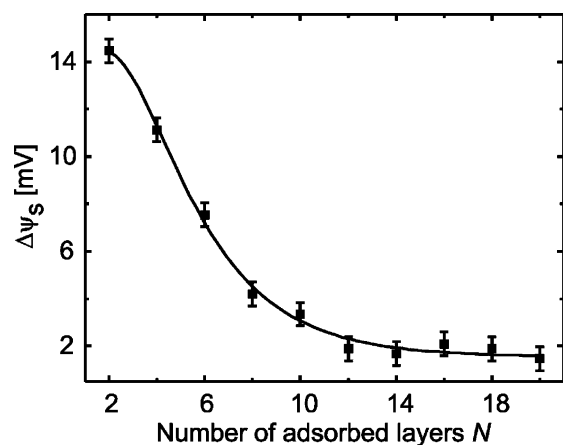
CDV

Figure 3. Potential change $\Delta\psi_S$ calculated from the measured change in sheet resistance is plotted as a function of the number of adsorbed monolayers N for PEMs deposited from 500 mM NaCl. Error bars are determined from the peak to peak noise of the measurement. Applying the capacitor model the solid curve was obtained from the fit by eq 1.
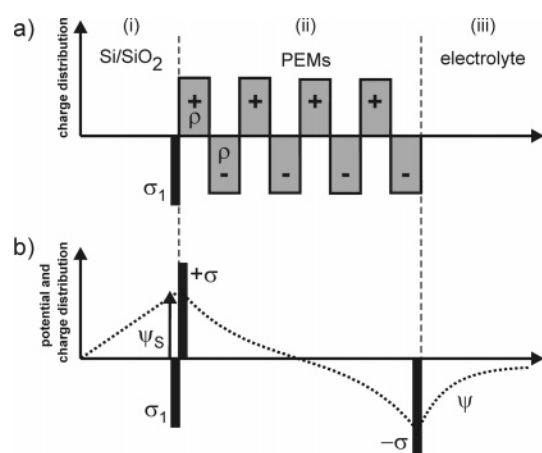

Figure 4. The system is modeled using three separate domains: (i) the Si/SiO$_2$ structure, (ii) the PEMs, and (iii) the electrolyte solution. The distribution of the immobile charges (the polyelectrolyte charges and the silicon oxide surface charge σ_1) is shown for two limiting cases: (a) separate layers inside the PEMs with a volume charge density ρ and (b) overlapping layers inside the PEMs with neutralized charges, except for the charges at the sensor surface and the PEMs/electrolyte interface with the surface charge density of $\pm(\sigma/2)$. Volume charges ρ are displayed in gray whereas surface charges σ are displayed in black. For case b the dotted line schematically shows the potential within the system. The potential ψ_S at the sensor surface is indicated.

we need to model the charge distribution within the PEMs. In general, the layers have a complex charge distribution due to, for example, interdigitation between polymers from adjacent layers. This overlapping of layers can even be of the same order as the layer thickness,[7] suggesting charge neutralization within the PEMs.[5] Therefore, we consider two limiting cases (Figure 4): (a) separate layers inside the PEMs with uniform volume charge density of $\rho = \pm\sigma/d$, where σ may be regarded as the surface charge density of each layer,[28] and (b) overlapping layers such that polyelectrolyte charges are completely neutralized within the PEMs, and thus the only uncompensated charges occur at the sensor surface and the PEMs/electrolyte interface with the surface charge density of $\pm\sigma/2$. Electrostatic screening by mobile charges is accounted for using the linear Debye–Hückel (DH) theory both within the PEMs medium (which is characterized by the screening length κ^{-1} and the dielectric constant ϵ) as well as in the diffuse electrical double layer of the electrolyte solution (which is characterized by the bulk screening length κ_0^{-1} and the dielectric constant for water ϵ_w).

One can thus identify characteristic Debye capacitances per area of $C_P = \epsilon\epsilon_0\kappa$ and $C_D = \epsilon_w\epsilon_0\kappa_0$ for the two media, respectively. The two models a and b considered for the limiting cases described above yield similar results for the behavior of ψ_S. On the linear Debye–Hückel level even identical results are obtained, indicating that the precise charge distribution within the PEMs is not a critical factor in our model (see Supporting Information). To compare our measurements with the model predictions, we calculate $\Delta\psi_S = \psi_S(N-1) - \psi_S(N)$ which can be simplified for $\kappa d \ll 1$ and even numbers of layers, N, yielding

$$\Delta\psi_S(N) = \frac{\sigma C_D^{-1}}{(C_S/C_P + C_P/C_D)\sinh(\kappa N d) + (1 + C_S/C_D)\cosh(\kappa N d)} \quad (1)$$

In eq 1 the number of layers, N, appears only in the hyperbolic functions. A value for the screening length κ^{-1} inside the PEMs can be obtained from the measured potential change $\Delta\psi_S(N)$ if the thickness d of the polyelectrolyte layers at a given ionic strength is known. Therefore, the monolayer thickness d was independently measured by ellipsometry. We found an average thickness of $d = 1.3 \pm 0.1$ nm for deposition from 50 mM and $d = 2.2 \pm 0.1$ nm for deposition from 500 mM bulk electrolyte solution, respectively. Selected ellipsometry data have been cross-checked by X-ray synchrotron reflectivity experiments,[18] confirming the obtained PEMs thicknesses. As can be seen in Figure 3, the measured $\Delta\psi_S$ can be fitted for κd by eq 1, yielding $\kappa^{-1} = 6.5 \pm 1.0$ nm for 500 mM bulk solution. A similar fit results in $\kappa^{-1} = 6.3 \pm 1.0$ nm for the buildup of the PEMs at 50 mM bulk solution. Equation 1 also provides an estimate for the surface charge density σ of the adsorbed polyelectrolyte layers, assuming that C_S is much smaller than C_D $(1 + C_S/C_D \approx 1)$. This leads to $\sigma = 0.020$ C/m^2 for the adsorption from 50 mM and $\sigma = 0.022$ C/m^2 from 500 mM bulk solution.

The relative dielectric constant ϵ of the PEMs can be calculated from κ, given the definition $\kappa^2 = 2N_Ae^2c/(\epsilon\epsilon_0 kT)$, where N_A is Avogadro's number, e is the elementary charge, c is the ion concentration, and k is the Boltzmann constant. For this, one has to determine the concentration c of mobile ions inside the PEMs, which is set by the thermodynamic equilibrium between the ions in the bulk solution (of concentration c_0) and those in the PEMs (see Supporting Information for details). It turns out that the dominant factor governing the ion partitioning in the PEMs/bulk electrolyte system is the Born energy change

$$\Delta\mu = \frac{e^2}{8\pi\epsilon_0 a}\left[\frac{1}{\epsilon} - \frac{1}{\epsilon_w}\right] \quad (2)$$

which arises because of the difference in self-energy of the ions (of radius a) in the PEMs and in the bulk leading to the well-known ion-partitioning law $c = c_0 \exp(-\Delta\mu/kT)$.[19,20] Combining the preceding relations and the definition of κ, the relative dielectric constant ϵ of the PEMs and the concentration of mobile ions can be calculated numerically from the values obtained for κ. We find $\epsilon = 30 \pm 2$ and $\epsilon = 21 \pm 1$ for the multilayers adsorbed from 50 mM NaCl and 500 mM NaCl, respectively. The corresponding concentration of mobile ions inside the PEMs is estimated to be of the order 0.9 ± 0.3 and 0.6 ± 0.2 mM, respectively.

A slightly higher value of $\epsilon = 50 \pm 10$ for the relative dielectric constant of PAH/PSS films has been estimated by comparing pyrene fluorescence data of the films with that of

CDV

various isotropic solvents of low molecular weight.[21] Durstock and Rubner[22] found dielectric constants by a factor 20 higher for PAH/PSS multilayers in water vapor. The large deviation from the values of the present paper is not fully understood. A possible explanation could be differences in swelling behavior in water vapor and liquid water as shown by neutron reflectometry.[23]

The different values for ϵ obtained for PEMs deposited from different salt concentrations can be interpreted in terms of a different water content of the polyelectrolyte films. A water content of about 40% was estimated by neutron reflectometry for PAH/PSS films deposited from different salt concentrations,[7,24-26] suggesting that the ionic strength of the solution does not change the water content of the PEMs. Assuming an equal water content for both salt concentrations, the observed variation of the dielectric constant could be ascribed to a different fraction of immobilized to free water within the polymer layers as oriented water molecules show a lower dielectric constant. Decreased water mobility inside PEMs has already been determined by NMR studies.[27] Comparing measurements at different conditions will be necessary to further determine the origin of the dielectric constants of PEMs.

Note that the DH approximation used in the present theoretical model is valid for relatively small electrostatic potentials. At room temperature, for symmetrical monovalent electrolytes this yields an upper limit of 50 mV, which is typically larger than the potentials measured in our experiments. In general, a full nonlinear Poisson–Boltzmann analysis would be necessary, which, however, is not analytically solvable for the present system. The main advantage of the DH approach lies in obtaining a simple analytical expression for the sensor device functionalized by PEMs enabling a direct comparison with the experimental data.

Conclusion. We were able to show that the recently introduced field effect device based on SOI is well suited for the quantitative determination of charge variations at complex interfaces. We apply a capacitor model including electrostatic screening by mobile charges within the PEMs to determine their dielectric constant as well as the concentration of mobile ions inside the polymer film. The origin of the dielectric constants found for PEMs deposited from different salt concentrations will need to be addressed further. The presented theoretical description, which is given here for the PEMs, may prove useful also for the quantitative analysis of differently functionalized field effect devices.

Supporting Information Available: Details of the capacitor models and the thermodynamic equilibrium between the ions in the bulk solution and the PEMs. This material is available free of charge via the Internet at http://pubs.acs.org.

References and Notes

(1) Decher, G. *Science* **1997**, *227*, 1232−1237.
(2) Bertrand, P.; Jonas, A.; Laschewsky, A.; Legras, R. *Macromol. Rapid Commun.* **2000**, *21*, 319−348.
(3) Farhat, T.; Yassin, G.; Dubas, S. T.; Schlenoff, J. B. *Langmuir* **1999**, *15*, 6621−6623.
(4) Sukhorukov, G. B.; Donath, E.; Lichtenfeld, H.; Knippel, E.; Knippel, M.; Budde, A.; Möhwald, H. *Colloid Surf., A* **1998**, *137*, 253−266.
(5) Schlenoff, J. B.; Ly, H.; Li, M. *J. Am. Chem. Soc.* **1998**, *120*, 7626−7634.
(6) Schmitt, J.; Grünewald, T.; Decher, G.; Pershan, P. S.; Kjaer, K.; Lösche, M. *Macromolecules* **1993**, *26*, 7058−7063.
(7) Lösche, M.; Schmitt, J.; Decher, G.; Bouwman, W. G.; Kjaer, K. *Macromolecules* **198**, *31*, 8893−8906.
(8) v. Klitzing, R.; Möhwald, H. *Langmuir* **1995**, *11*, 3554−3559.
(9) Schollmeyer, H.; Daillant, J.; Guenoun, P.; v. Klitzing, R., in preparation.
(10) Slevin, C. J.; Malkia, A.; Liljeroth, P.; Toiminen, M.; Kontturi, K. *Langmuir* **2003**, *19*, 1287−1294.
(11) Pouthas, F.; Gentil, C.; Cote, D.; Zeck, G.; Straub, B.; Bockelmann, U. *Phys. Rev. E* **2004**, *70*, 031906.
(12) Fritz, J.; Cooper, E. B.; Gaudet, S.; Sorger, P. K.; Manalis, S. R. *Proc. Natl. Acad. Sci. U.S.A.* **2002**, *99*, 14142−14146.
(13) Uslu, F.; Ingebrandt, S.; Mayer, D.; Böcker-Meffert, S.; Odenthal, M.; Offenhäusser, A. *Biosens. Bioelectron.* **2004**, *19*, 1724−1731.
(14) Nikolaides, M. G.; Rauschenbach, S.; Luber, S.; Buchholz, K.; Tornow, M.; Abstreiter, G.; Bausch, A. B. *ChemPhysChem* **2003**, *4*, 1104−1106.
(15) Nikolaides, M. G.; Rauschenbach, S.; Bausch, A. B. *J. Appl. Phys.* **2004**, *95*, 3811−3815.
(16) Siu, W. M.; Cobbold, R. S. C. *IEEE Trans. Electron Dev.* **1979**, *ED-26*, 1805−1815.
(17) Netz, R. R.; Joanny, J.-F. *Macromolecules* **1999**, *32*, 9013−9025.
(18) Reich, C.; Hochrein, M.; Krause, B.; Nickel, B. *Rev. Sci. Instrum.* **2005**, *76*, 095103.
(19) Israelachvili, J. N. *Intermolecular and Surface Forces*; Academic Press: London, 1991.
(20) Netz, R. R. *Eur. Phys. J. E* **2000**, *3*, 131−141.
(21) Tedeschi, C.; Möhwald, H.; Kirstein, S. *J. Am. Chem. Soc.* **2001**, *123*, 954−960.
(22) Durstock, M. F.; Rubner, M. F. *Langmuir* **2001**, *17*, 7865−7872.
(23) Steitz, R.; Wong, J. E.; v. Klitzing, R., unpublished results.
(24) Steitz, R.; Leiner, V.; Siebrecht, R.; v. Klitzing, R. *Colloid Surf., A* **2000**, *163*, 63−70.
(25) Wong, J. E.; Rehfeldt, F.; Haenni, P.; Tanaka, M.; v. Klitzing, R. *Macromolecules* **2004**, *37*, 7285−7289.
(26) Carriere, D.; Krastev, R.; Schönhoff, M. *Langmuir* **2004**, *20*, 11465−11472.
(27) Schwarz, B.; Schönhoff, M. *Langmuir* **2002**, *18*, 2964−2966.
(28) A mesh size of ≈30 nm can be estimated for the adsorbed polyelectrolyte layers.[17] This mesh size is smaller than the estimated effective persistence length of PSS (≈100 nm), suggesting that alternating polyelectrolyte layers form with charge densities which are equal in magnitude.

MA0519213